AUGMENTATION OF SOLAR STILL PERFORMANCE USING FLASH EVAPORATION

تحفيز أداء المقطر الشمسى باستخدام التبخير الوميضى

A.M. El-Zahaby*, A.A. Kabeel*, A.I. Bakry*, S. A. El-agouz*, and O.M. Hawam**

* Mechanical Power Department, Faculty of Engineering, Tanta University, Egypt

** Workers University, Mansoura, Egypt

ملخص البحث

يقدم هذا البحث تطبيق جديد في مجال تحلية المياه. حيث يتم التقطير باستخدام الغازات الساخنة كمصدر للحرارة وذلك من خلال تعديلات في تصميم المقطر الشمسي التقليدي وذلك باستخدام حوضاً متدرجاً للمياه ونظام لرش المياه تعتمد على موتور كهربائي صغير لتحريك رشاشات المياة. تمت هذه التعديلات بهدف الإستفادة من غازات العادم الناتجة من مصادر عديدة مثل محطات توليد الكهرباء. تمت دراسة تأثير درجة حرارة دخول المياة العكرة عند سرعة دوران (250 لفة/دقيقة) للموتور و معدل تدفق (4 لتر/ساعة) للمياة وكذلك تم دراسة تأثير معدلات مختلفة لطاقة الغازات الساخنة عند سرعتي دوران 100 , 250 لفة/دقيقة للموتور ومعدلات تدفق 9.333 , 4.0 , 3.635 لتر/ساعة لدخول المياه. وقد تبين أن أداء المقطر الشمسي يقل بزيادة درجة حرارة دخول المياة. كما تبين أن معدل أنتاجية المياه المقطرة قد يصل إلى حوالي (54.5 لتر/م². يوم) بكفاءة حرارية (50.03%) وذلك عند ظروف تشغيل (250 لفة/دقيقة، معدل تدفق 9.333 لتر/ساعة ، معدل إستهلاك طاقة مقدارة 2.919 ك.وات، درجة حرارة القاعدة 76.7 م°، درجة حرارة سطحي الغطاء الداخلي والخارجي 53.6 , 35.9 م° على الترتيب ودرجة حرارة دخول المياه 28.7 م° ودرجة حرارة الجو 32.3م° وكانت سرعة الرياح 0.9 م/ث).

Abstract

A new design of a stepped solar desalination system with flashing chamber is experimentally investigated. The main objective of the investigation was to study the performance of step-wise water basin coupled with a spray water system by augmenting desalination productivity through using two air heaters. The effect of using the spray system for seawater is investigated experimentally at different velocities of the water spray's holder and flow rates on the performance of the solar still in a previous article by the authors [1]. In the present article the effect of the inlet raw water temperature (at motor speed of 250 rpm and water flow rate of 4 l/h) and the power consumed by the two air heaters (at both 100 and 250 rpm and water flow rates 3.635, 4.0 and 9.333 l/h) on the performance of the proposed solar system are investigated. It was found that the productivity and performance of the system were significantly positive dependent on both inlet impure water temperature and the power consumed. They decrease with the increase of inlet impure water temperature. At 250 rpm the productivity and efficiency increases with the power consumed to a certain limits after which they begin to decreases gradually while at 100 rpm the productivity and so the efficiency decreases with the power consumed gradually.

1. Introduction

The increasing population and industrial agricultural development of rural areas are creating an unbalance between drinking water demand and fresh water supply. It is well known that solar desalination exhibits considerable economic advantages over other salt water desalination processes because of cost-free energy, reduced operating costs and its simple structure. Though, many investigators studied the effect of different factors such as solar radiation, ambient temperature, water depth, and wind velocity, on the performance of the still. For most cases, even under optimized operating conditions, the reported efficiency of the single basin solar still was in the range of 30-45%, with less than 5 l/m^2.day of fresh water production. This low efficiency is mainly due to the complete loss of latent heat of condensation of water vapor on the glass cover of the solar still. Multi-effect solar stills are used to improve production of desalinated water but only in small capacities because the condenser is an integral part of the still. The low heat and mass transfer coefficients in this type of stills require operation at relatively high temperatures and thus the use of large, expensive, metallic surfaces for evaporation and condensation. A

solar still, with its lower productivity, does not compete with other desalination techniques. However, when the demand of fresh water does not exceed a few cubic meters, the solar still is a viable option. Since the productivity of the solar still increases as the saturation pressure of the water increases, this is determined by the temperature at the brine surface.

A.Rahim [2] introduces a new technique developed to improve the efficiency of both evaporating and condensing zones, and concluded that:

. Separating the evaporator and condenser in two different units allows the temperature difference between the evaporator and condenser zone to be controlled independently to a relatively large amounts during the day.

As the potable water is collected in the condenser unit, the re evaporation of the condensed potable water is eliminated.

Chen Ziqian, et al [3] developed and tested a special desalination unit which utilizes solar or waste energy. He concluded that by the simulation of his unit operating with a solar system under practical weather conditions, the yield rate of the unit is more than two times

comparing with that of a conventional single basin type of solar still.

Imad Al-Hayek et al [4] was found that the distilled water output of the asymmetric green house type was 20 percentages higher than that of symmetric greenhouse type.

Guofeng Yuan et al [5] concluded that:

For a fixed solar area (absorber), the increase in feed water flow rate will decrease fresh water production because of the spray temperature decrease

The matching of the cooling water flow rate with the collector area is very important to obtain maximum fresh water production.

The year-round study shows that in (xi'an china), 5.2 kg/m^2.day can be obtained in June. In December, 2.7 kg/m^2.day can be reached.

A numerical study was carried out by Hassan E.S.Fath et al [6] to investigate the thermal performance of a new still. The results show that: The still productivity is about 5.2 kg/m^2.day, and decreasing air flow rate has insignificant influence on the productivity.

For an innovative water desalination system using low grade solar heat , S. Al-Kharabsheh et al [7] concluded that : the performance of this system is superior to a flat basin solar still , and the output may be twice that of a flat basin type for the same input.

A solar still with a concave wick evaporation surface was fabricated and tested by A.E. Kabeel [8]. The average daily efficiency was calculated as 30 percentages and the average productivity in day time was 4.1 l/m^2.

B. Janarthanan et al [9] proposed a floating cum tilted wick type solar still with flowing water over the glass cover. They have concluded the followings:

Glass cover temperature decreases significantly due to the water flowing over the glass cover which causes fast evaporation during peak sunny hours.

The effect of water flowing over the glass cover has a fascinating role on the performance of the still.

Hiroshi Tanaka et al [10] investigated theoretically a vertical multiple-effect diffusion-type solar still. It was found that:

The overall daily productivity is larger for the optimum solar collector angle stills than the fixed one on the summer or winter solstices.

The productivity increases with a decrease in the feed rate of saline water to the wicks

To increase the productivity, a simple device such as a black tube can be used to increase the feeding temperature of saline water to the wicks.

Zeinab S. Abdel – Rahim [11] designed a modified solar desalination

system. It has two modifications; the first one is a backed layer. The second modification is the using rotating shaft installed close to the basin water surface. Based upon the results obtained from the comparisons between the two modified stills and a conventional type, the following conclusions were reached:

. The overall efficiency of two modified systems was higher than the conventional type.

. Modified solar desalination system used packed layer had higher productivity than that one used rotating shaft and both are better than the conventional type.

Y. J. Dia et al [12] tested a solar desalination unit with a humidification and dehumidification (HDD) cycle. The unit improved the effect of evaporation and overcame the difficulty of increasing the evaporation temperature and decreasing the condensation temperature at the same time by using a falling film humidifier with large evaporation surface and forced convection to enhance the heat and mass transfer. The thermal efficiency of the system is about 0.85 under optimal operating conditions.

J.Orfi [13] studied theoretically a solar desalination system with HDD. He said that the daily production of fresh water depends on the ratio between the salt water and the air mass flow rates. It was found that this desalination unit can produce fresh water at high rates (more than 15 L/m^2.day).

Zheng Hongfei et al [14] constructed and tested an indoors active regenerative solar still with an area of 1.03 m^2. He concluded that the performance ratio is about two to three times greater than that of a conventional basin-type solar still.

Ali A. Badran [15] studied a single-stage, basin-type solar still connected with a conventional flat-plate collector. He reports that the productivity of the system was substantially increased in comparison with that of the still alone. Mean while efficiency was reduced by a few percentage points.

Adel K. El-Fiqi et al [16] studied an extensive experimental work on the flashing process using fresh liquid. The work concerned the spray flash evaporation occurring in superheated water. Jet was injected through circular nozzles into a low-pressure vapor zone. The results showed that:

Increasing the degree of superheat leads to an increase in the flashing vapor to a certain amount.

With the increase of the degree of superheat, both the flashing efficiency and the flashed vapor increase.

. Decreasing the water level inside the flash chamber increases slightly both the

flashing efficiency and the amount of the flashed vapor.

K. Voropoulos et al [17] and E. Mathioulakis et al [18] designed and investigated a solar still-storage tank system. It has been shown that this design leads to higher distilled water output. The proposed solar distillation system concerns finally a hybrid design from the usage point of view and from the heat source point of view. It can exploit not only solar energy incident on saline water but also any other heat source available nearby , such as waste heat , conventional sources, electricity , solar collectors , solar pools , etc.

A. E. Kabeel et al [19] concluded that the use of corrugated wick surface increases the output of the roof type solar still. The productivity of the system is enhanced with about 30%.

2. Experimental Setup

The solar desalination system under study sprays impure water with definite different flow rates is schematically shown in Fig. (1.a). This system includes stepped basin still; Fig. (1.b), with 10 steps; which represents the absorber with area of 1.0 m² (1.54×0.65 m²). Higher side and the two similar sides are constructed from 2 mm blackboard coated iron while the casing is constructed from 0.8 mm galvanized

steel. The stepped-bed, higher side and the two sidewalls of the still are insulated with 30 mm glass wool (thermal conductivity of 0.036 W/m K) while the front wall (lower side) was normal to the bed and is made of a plastic sheet 3 mm thickness in an aluminum frame like the cover. The main condenser is the still body cover, which made of 3 mm plastic sheet thickness (1.54×1.06 m²) in an aluminum frame. There is a secondary condenser which constructed from 0.8 mm galvanized steel (1.3×0.1×0.4 m³) and 9 copper tubes 6.35 mm in diameter and 1.3 m length. The system includes two water loops. The 1st (main) loop is used for injecting impure water in the flash chamber (evaporation area). It consists of water supply tank, 3 kW water type electric heater (149W only consumed) water flow meter (orifice meter), controlling valves, and 3 sprayers. These sprayers could be modified to provide a variety of profiles but only one set is used during all experiments. The exit diameter of the spray nozzles is about 1.25 mm. A special mechanism for moving the sprayer's holder in a reciprocating linear motion is designed and constructed. The mechanism converts the rotary motion of 0.37 kW electric motor to a reciprocating linear motion with the required speed; (but the actual consumed power

dependent the water flow rate and the rotating speed) as an example for water flow rate = 6. 635 l/h and rotating speed = 250 rpm the consumed power = 51.2 W. The test loop is designed to work with a flow range of 0 to16 l/h, and an electric motor speed range 0 to 350 rpm which is corresponding to the reciprocating speed 0 to 0.0237 m/s as shown in table 1.

Table 1 the corresponding reciprocating speed to the motor speed

rpm	100	150	200	250	300	350
cm/s	0.628	0.977	1.313	1.625	2	2.364

Figure (2) shows a photo of the designed solar still with the storage tank coupled with the electric motor. The second loop is used to condense, collect and measure the flashed vapor. It consists of the still body plastic cover (main condenser), fresh water trough, rubber tube and graduated vessel. Finally the system includes one hot air (or gases) loop. It is used for circulating hot air (gases) under the stepped base of the still. It consists of a 0.5 hp centrifugal fan, air flow meter (orifice meter), controlling valve, U tube manometer and two electrical heaters (the power of each one is 2 kW). Figure (3) shows a photo of the designed solar still with the hot air loop. The entire test facility was

constructed of iron tubes and elbows 1.27, 3.81 and 5.08 mm in diameter, stainless steel tube 12.5 mm in diameter, copper tubes 6.35 mm in diameter and rubber tubes.   Impure water is continually sprayed at a defined constant flow rate through the nozzles to form falling scattered small drops on the heated stepped basin (absorber). Because of the flash evaporation and mass exchange between impure water and air, the vapor condenses mainly on the inner cover surface and secondarily (partially) in the condenser unit, turning into fresh water. The remaining impure water is drawn continually by gravity.

3. Instrumentation

The temperatures at different points in the system are measured by T-type thermocouples, 0.5 mm diameter. There are twelve thermocouples located at the base of the still, two thermocouples on the inner cover surface (condenser) and other two thermocouples on the outer cover surface. All the thermocouples were calibrated in hot water bath with the aid of a standard thermometer. Through a multi- point switch, the thermocouples are connected to a digital thermometer type BK precision 922 of an accuracy ±0.1 °C.   With a standard K-type thermocouple, the BK precision 922 is capable of temperature measurements in

the range of −20 °C to +1370 °C. Finally, the solar radiation is measured by using of both TD 208 b-solar meter and a silicon cell pyranometer model 3120 of an accuracy ±1 W/m². Moreover, the wind speed was measured by an anemometer (digital turbofan, TFA) of an accuracy ±0.1 m/s. The productivity is measured by graduated vessel 1000 ml plus or minus 10 ml (± 1 %).

4. Experimental Procedure

The experimental tests of this work were conducted at Tanta University, Egypt. There are two groups of the experiments; the first one had been finished during the period from 12 to 15 August 2008, and the second group had been done during the period from 5 September to 15 November 2008 and from 31 May to 14 June 2009. In the first group each experiment was conducted in one day, during which the following measurements had been recorded:

- Basin (absorber) local and mean temperatures.
- Outer and inner plastic cover (main condenser) temperatures.
- Productivity.
- Total solar radiation intensity, as usual on a horizontal plane.
- Ambient air temperature and wind speed.

The experimental data are collected at regular intervals of one hour, starting from about 9 a.m. up to the sunset.

In the second group the following measurements have been recorded:

* Steady state basin (absorber) local and mean temperatures.

* Outer and inner plastic cover, ambient air and inlet raw water temperatures.

* Inlet and outlet (exhaust) hot air temperatures. The air manometer head; from which the power consumed can be calculated.

* Productivity.

The experimental data are collected at regular intervals of half hour after reaching to steady state.

5. Results and Discussion

Results for different experiments are given in graphical form in order to simplify the discussion. The experimental results of the present work are divided into two groups.

The first group concerns with the effect of inlet raw (impure) water temperature; which can be controlled by using of 3 kW electric water heater (149W only consumed) and thermostat at constant flow rate of the impure water (4.00 l/h) and constant motor speed (250 rpm) on the system performance. The

experiments are carried out during the period from 12 to 15 August 2008.

In particular (premenarly), we consider processes that can occur at a solid-liquid interface, namely, boiling and condensation. For these cases, latent heat effects associated with the phase change are significant. The change from the liquid to the vapor state due to boiling is sustained by heat transfer from the solid surface. Because there is a phase change, heat transfer to the fluid can occur without influencing the fluid temperature. In fact, the evaporation process occurs when the temperature of the surface T_s exceeds the saturation T_{sat} corresponding to the liquid pressure. Heat is transferred from the solid surface to the liquid, and the appropriate form of Newton's law [20] was applied.

The process is characterized by the formation of vapor bubbles, which grow and subsequently detach from the surface. Vapor bubble growth and dynamics depend, in a complicated manner, on the excess temperature (T_s - T_{sat}), the nature of the surface, and thermo physical properties of the fluid, such as its surface tension σ. In turn, the dynamics of vapor bubble formation affect fluid motion near the surface and therefore strongly influence the heat transfer coefficient [20].

Figure 4 (a, b) shows the variation of the hourly and accumulated productivities for different inlet raw (impure) water temperature. From the figure it can be seen that, both the hourly and accumulated productivities decrease with the increase of the inlet raw water temperature. It can be said that this is because of the heat transfer from the solid surface (absorber) to the liquid (water droplets) is proportional to (affected with) the excess temperature (ΔT_e); where ΔT_e =T_S-T_{sat} , T_s is the surface (absorber) temperature and T_{sat} is the saturation temperature corresponding to the liquid pressure; where the appropriate form of Newton's low of cooling is: $q^{"}$=h(T_S-T_{sat}) [20]. The heat transfer coefficient strongly influenced by the nature of the surface, thermo physical properties of the fluid, such as its surface tension and the dynamics of vapor bubble formation [20]. Accumulated productivity reaches about 2 times of the traditional type at the same time of the year (water depth 3 cm), [21].

Figure 5 (a, b, c) shows the variation of base temperature, inner and outer cover temperatures with time during the day time. From this figure it can be seen that: the base and consequently, inner and outer cover temperatures increase with time starting from sunshine hour,

reaches its maximum value around the noon time and then decreases gradually. The differences in the base temperature and consequently, the inner and outer cover temperature for the different inlet raw water temperature reach its maximum value (about 6, 9, and 12 °C) respectively around 1 pm.

Figure 6 (a, b) shows the variation of both solar radiation and ambient air temperature respectively along the day during the 1st group measuring period. It can be seen that: 1- both solar and ambient air temperature increase up to 12 o'clock, and then decrease gradually.
2- the coincidence of both the solar radiation and ambient air temperature values for the different days is shown.

The variation of both the average daily efficiency and daily productivity with the impure water temperature are shown in Figure 7 and 8, respectively. It is clear that the average daily productivity and consequently efficiency, decrease with the increase in impure water temperature. The hourly and daily efficiencies may be calculated from the following equations, [8]. The power consumed by water electric heater and the electric motor was about 200W and maybe neglected.

$$\eta_h = \frac{M_w \, L_{w \cdot av}}{3600 \, A_b \, H} \qquad (1)$$

$$\eta_d = \left(\frac{1}{n}\right)\left(\sum_{i=1}^{n} \eta_{hi}\right) \qquad (2)$$

where M_w is the hourly productivity (kg/h), $L_{w.av}$ is the hourly average of the latent heat of vaporization of water (J/kg), A_b is the basin area (1.0 m^2), H is the incident solar radiation on the horizontal surface (W/m^2), and n is the number of desalination hours.

The second group of experiments deal with the influence of the power consumed by the hot air under steady state conditions (constant base temperature) on the performance of the system for two constant motor speeds (250 and 100 rpm) at different three water flow rates (9.333. 4.000 and 3.635 l/h).

The experimental data are collected and represented through four graphs from figure 9 to figure 12.

Figures (9) shows the relation between system productivity (l/h) and power consumed (kW) at 250 rpm for the three different water flow rates (9.333, 4000 and 3.635 l/h). From this figure, generally it can be seen that:
The productivity increases with the power consumed to a certain limits after which it begins to decrease.

Figure (10) shows the relation between the system productivity (l/h) and power consumed (kW) at 100 rpm for the three different water flow rates (9.333, 4.000 and 3.635 l/h). From this figure it can be said that:

In general, the productivity decreases with the increase of the power consumed. Any other points irrespective of this will

Water flow rate	Motor speed 250 rpm			Motor speed 100 rpm		
	a	b	c	a	b	c
9.333	-0.9288	5.3037	-7.0631	0.2407	-1.6761	3.2721
4.000	-0.1678	1.0476	-1.2413	-0.0617	0.2904	0.0235
3.635	-0.1404	0.5953	-0.1161	0.1415	-1.0388	2.1500

be attributed to the difference between the base and cover temperatures and the difference between inner and outer cover temperatures.

Figure (11) shows the relation between system efficiency and the power consumed (kW) at 250 rpm for the three different water flow rates (9.333, 4000 and 3.635 l/h). From this figure generally it can be seen that:

The efficiency increases with the increase of the power consumed to a certain limit after which it begins to decrease.

Figure (12) shows the relation between system efficiency and the power consumed (kW) at 100 rpm for three different water flow rates (9.333, 4.000 and 3.635 l/h). From this figure it can be

said that, generally, the system efficiency decreases with the increase of the power consumed.

Referring to figures (11 and 12) the system efficiency can be expressed by equation (3), with a maximum error 13.196% for motor speed 250 rpm and 13.46% for motor speed 100 rpm.

$$\eta = a \times Q^2 + b \times Q + c \qquad (3)$$

where;

Q: is the power consumed (kW).

The constants a, b and c are tabulated in the shown table;

Conclusions

An extensive experimental investigation on a stepped solar still augmented with hot water storage tank and two electrical air heaters using flash evaporation was carried out. The work was concerned with the variation of the inlet water impure temperature ranges between (40-60°C), power consumed at steady state condition (constant base temperature). The results show that:

- Increasing the inlet impure water temperature leads to a decrease in the flashing vapor (productivity), and so the system efficiency.

- The desalination (productivity) augments through using two air

heaters (power consumed), whereas the following conclusions are reached:

- In the investigated limits, at 250 rpm the system productivity and efficiency increase with the increase of the power consumed to a certain limits after which they begin to decrease gradually.

- In the investigated limits, at 100 rpm the system productivity and efficiency decrease with the increase of the power consumed.

- For definite conditions (250 rpm, water flow rate = 9.333 l/h, power consumed = 2.9199 kW, base temperature = 76.7 °C, inner cover temperature =53.6 °C, outer cover temperature = 38.9 °C, inlet water temperature = 28.7 °C, ambient air temperature = 32.3 °C.and wind speed = 0.9 m/s) the productivity reaches 2.27 l /m^2.h; ie 54.48 l/m^2.day with a thermal efficiency 0.50026.

References

[1] A.M El-Zahaby , A.A Kabeel , A.I. Bakry , S.A. El-agouz , and O.M Hawam "Enhancement of solar desalination still productivity using flash evaporation" MEJ, vol .34, No. 1, March 2009.

[2] Nabil Hussain A. Rahim, "Utilisation of new technique to improve the efficiency of horizontal solar desalination still", Desalination 138 (2001)121-128.

[3] Chin Ziqian, Zeng Hongfei, He Kaiyan, Ma Choachen, "steady-state experimental studies on a multi-effect thermal regeneration solar desalination unit with horizontal tube falling film evaporation", Desalination 207 (2007) 59-70.

[4] Imad Al-Hayek, Omar O. Badran,"The effect of using different designs of solar stills on water distillation", Desalination 169 (2004) 121-127.

[5] Guofeng Yuan, Hefei Zhang, "Mathematical modeling of a closed circulation solar desalination unit with humidification-dehumidification" Desalination 205 (2007) 156-162.

[6] Hassan E. S. Fath, Samy M. El-Sherbiny, Ahmad Ghazy, "Transient analysis of a new humidification-dehumidification solar still", Desalination 155 (2003) 187-203.

[7] S Al-Kharabsheh, D. Yogi Goswami, "Analysis of an innovative water desalination system using low-grade solar heat", Desalination 156 (2003) 323-332.

[8] A.E. Kabeel, " Performance of solar still with a concave wick evaporation surface", Energy xxx (2009) 1-6.

[9] B. Janarthanan, J. Chandrasekaran, S. Kumar, "Performance of floating cum tilted-wick type solar still with the effect

M. 27

of water flowing over the glass cover", Desalination 190 (2006) 51-62.

[10] Hiroshi Tanaka, Yasuhito Nakatake, Katsuhiro Watanabe, "Parametric study on a vertical multiple-effect diffusion-type solar still coupled with a heat-pipe solar collector", Desalination 171 (2004) 243-255.

[11] Zienab S. Abdel-Rehim, Ashraf Lasheen, "Improving the performance of solar desalination systems", Renewable Energy 30 (2005) 1955-1971.

[12] Y. J. Dai, H. F. Zhang, "Experimental investigation of a solar desalination unit with humidification and dehumidification", Desalination 130 (2000) 169-175.

[13] J. Orfi, N. Galanis, M. Laplante, "Air humidification --dehumidification for a water desalination system using solar energy", Desalination 203 (2007) 471-481.

[14] Zheng Hongfei, Ge Xinshi, "Steady-state experimental study of a closed recycle solar still with enhanced falling film evaporation and regeneration", Renewable Energy 26 (2002) 295-308.

[15] Ali A. Badran, Ahmad A. Al-Hallaq, Imad A. Eyal Salam, Mohammad Z. Odat, "A solar still augmented with a flat-plate collector", Desalination 172 (2005) 227-234.

[16] Adel K. El-Fiqi, N.H. Ali, H.T. El-Dessouky, H.S. Fath, M.A. El-Hefni,

A.M. El-Zahaby, A.A. Kabeel, A.I. Bakry, S.A. El-agouz and O.M. Hawam "Flash evaporation in a superheated water liquid jet", Desalination 206 (2007) 311-321.

[17] K. Voropoulos, E. Mathioulakis, V. Belessiotis, "Experimental investigation of the behavior of a solar still coupled with hot water storage tank", Desalination 156 (2003) 315-322.

[18] E. Mathioulakis, V. Belessiotis, "Integration of solar still in a multi-source, multi-use environment", Solar Energy 75 (2003) 403- 411.

[19] M. M. Bekheit, A. E. Kabeel, E. A. El-Negiry and A. M. Hamed, "Theoretical and experimental investigation of a roof-type solar still augmented with corrugated wick of cloth layer", 12th International Mechanical Power Engineering Conference, Mansoura, Egypt, (2001) 73-85.

[20] Fundamental of heat and mass transfer, Frank P. Incropera and David P. Dewitt, fourth edition.

[21] M.S. Abdel Salam, H.E. Gad, M.A. Tolba and O.M. Hawam "Effect of cover slope on the thermal performance of the basin-type solar still", MEJ, vol.18, NO.1, March 1993.

Nomenclature

A_b Base area, m^2

H Hourly solar intensity, W/m^2

h Convection coefficient $W/m^2.°C$

$L_{w,av}$ Latent heat of water at average base temperature, kJ/kg

M_w Hourly productivity, mL/h

n   Number of sunshine hours, h

$q^{''}$ Heat transferred from the solid surface to the liquid, W/m^2.

T_s Surface temperature, $^\circ$K.

T_{sat} Saturation temperature corresponding to the liquid pressure, $^\circ$K.

η_d Average daily efficiency.

η_h Hourly efficiency

1- Impure water inlet pipe.
2- Impure water tank.
3- Water type electric heater.
4- Water orifice meter.
5- Stepped solar still.
6- Productivity tube.
7- Graduated flask
8- Control valves.
9- Measument instromentation.
10- Hot air dual system.
11- Air type electric heater.
12- to manometer.
13- Air orifice meter.
14- Air blower.
15- Feeding spray nozzles.
16- Nozzles holder.
17- Plastic cover 3 mm thickness (main condenser).
18- secondary condenser.
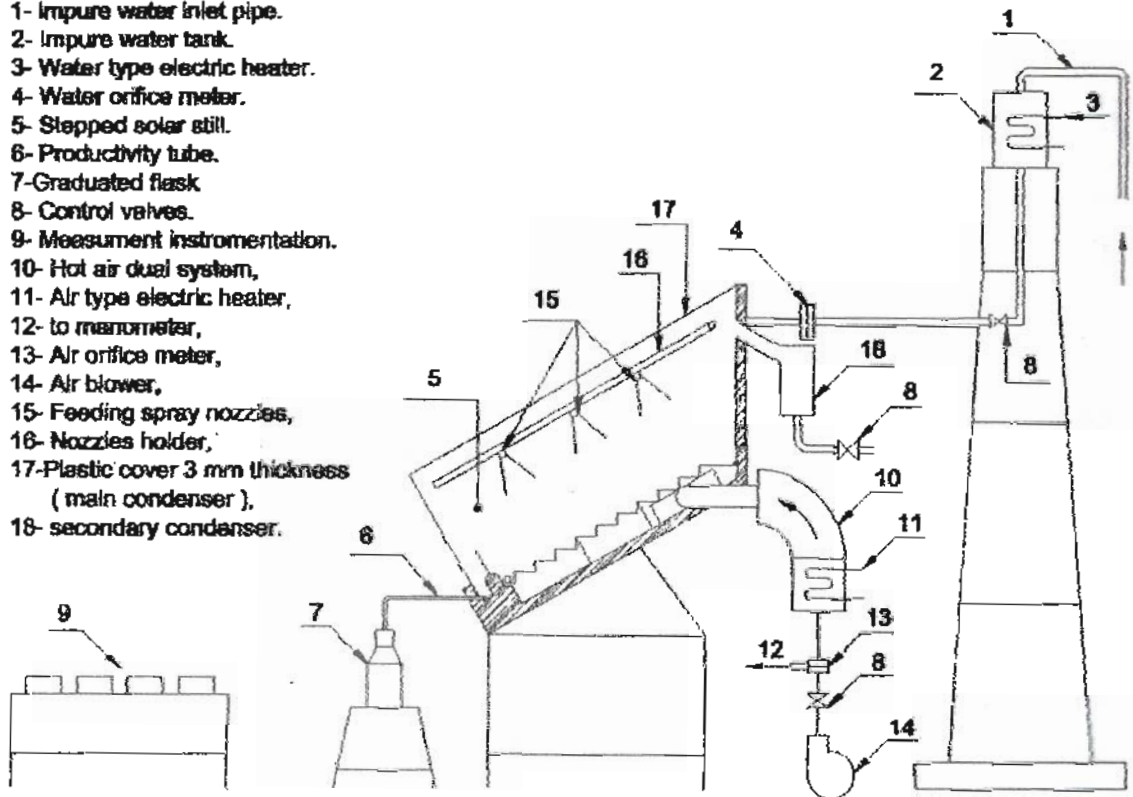
Figure 1.a Schematic diagram of the setup.

Figure 1.b Schematic diagram and dimensions of the stepped solar still (test section)

Figure 2 A photo of the designed solar still with the storage tank.

Figure 3 A photo of the designed solar still with the hot air loops.

a)

b)
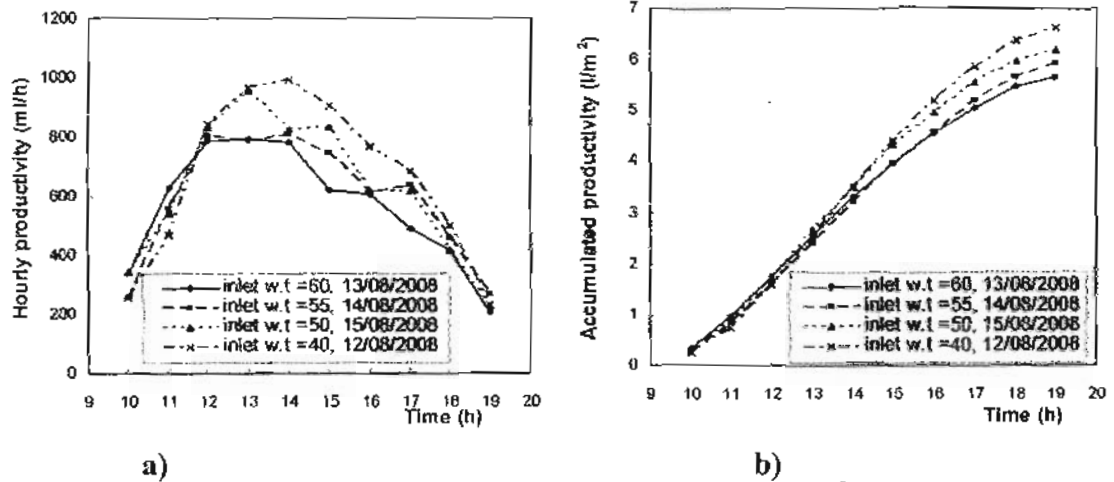
Figure (4) Hourly (ml/h) and accumulated productivity (l/m^2) along the day time for different inlet raw water temperatures at water flow rate =4 l/h and 250 rpm.
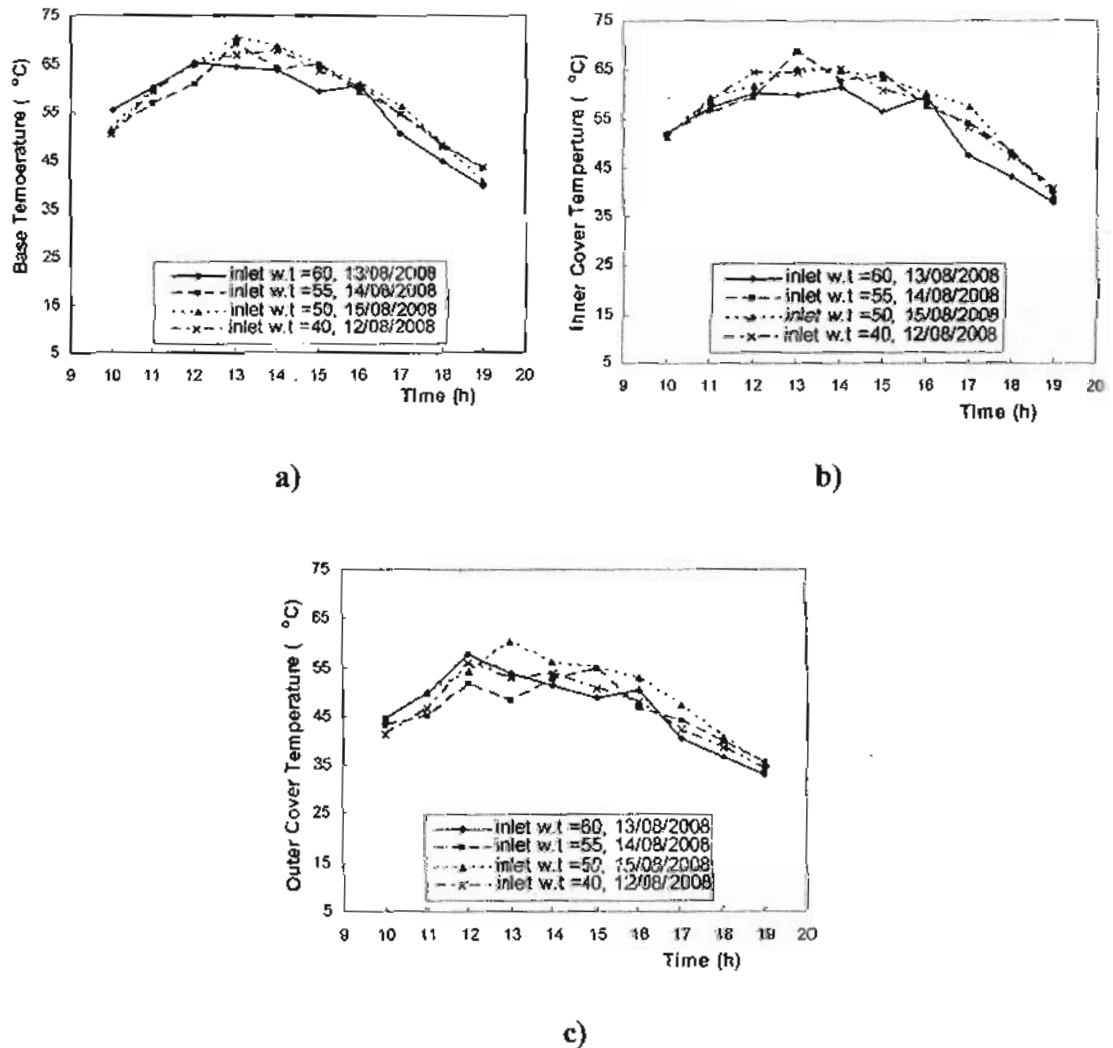

a)

b)

c)

Figure (5) variation of base, inner and outer cover temperature ($^\circ$C) along the day time for different inlet raw water temperatures at water flow rate =4 l/h and 250 rpm.

a)   b)
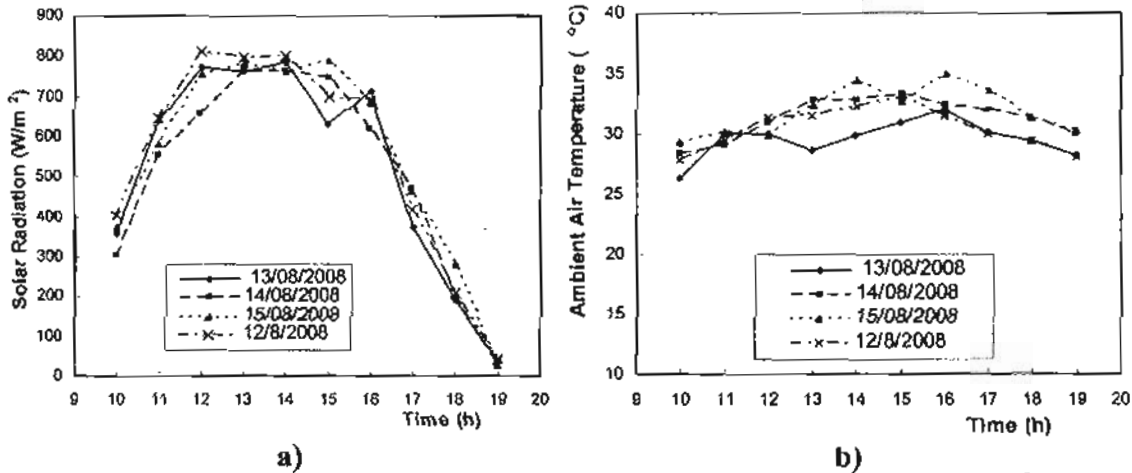
Figure (6) Variation of solar radiation and ambient air temperature ($^\circ$C) along the day time during the 1st group experiment period at water flow rate =4 l/h and 250 rpm.
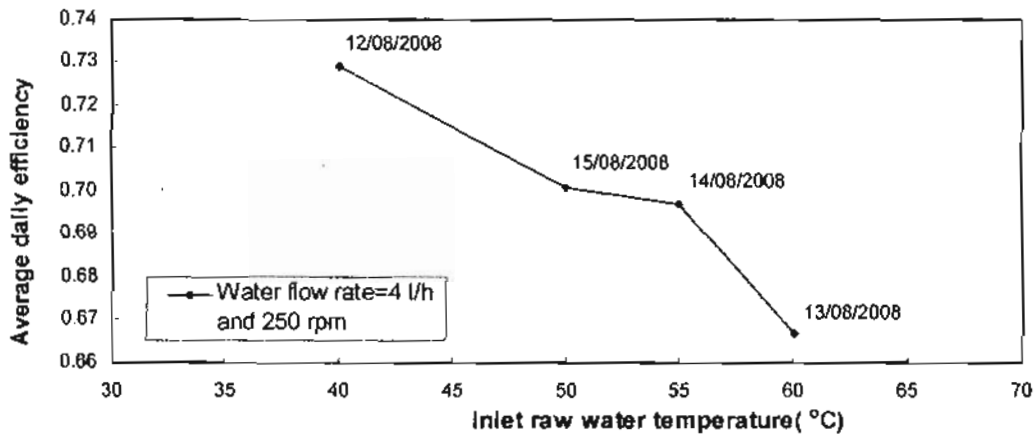
Figure (7) Variation of the average daily efficiency for the different impure water temperature
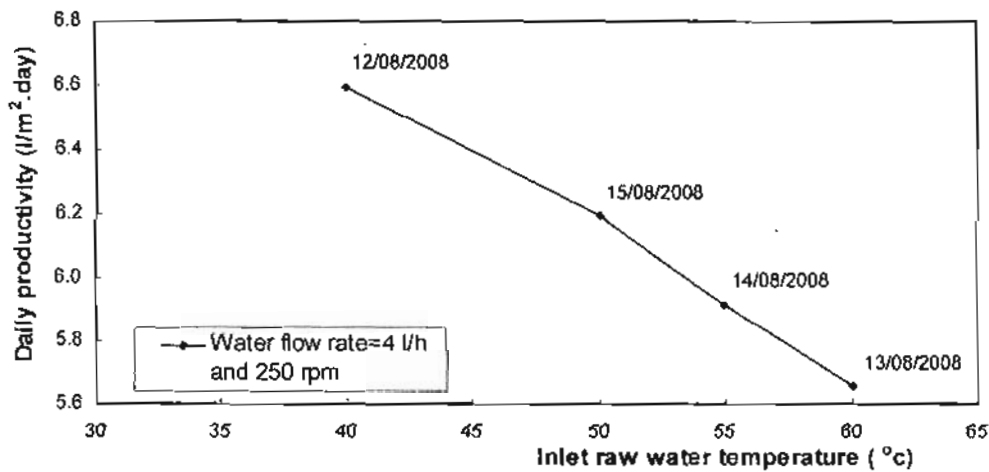
Figure (8) Variation of accumulated productivity for the different impure water temperature
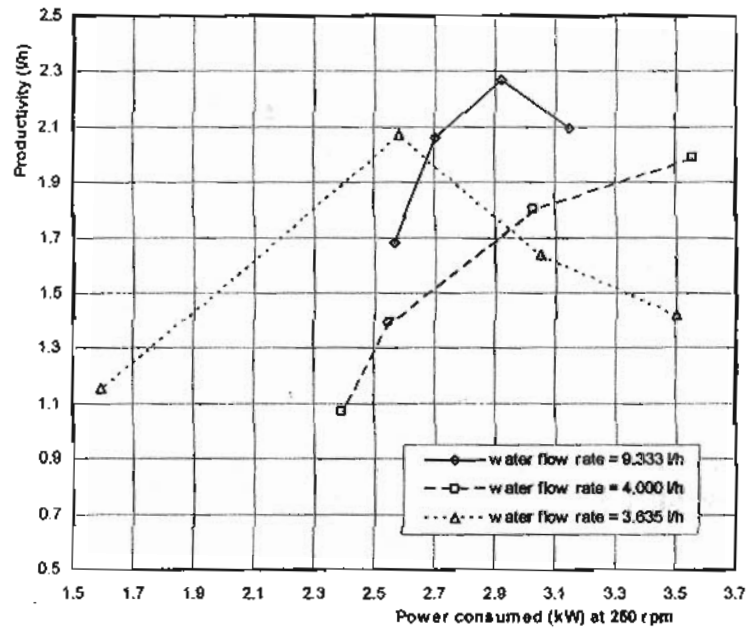
Figure (9) Variation of the system productivity with the power consumed, at 250 rpm for different water flow rates = 9.333, 4.000 and 3.635 l/h
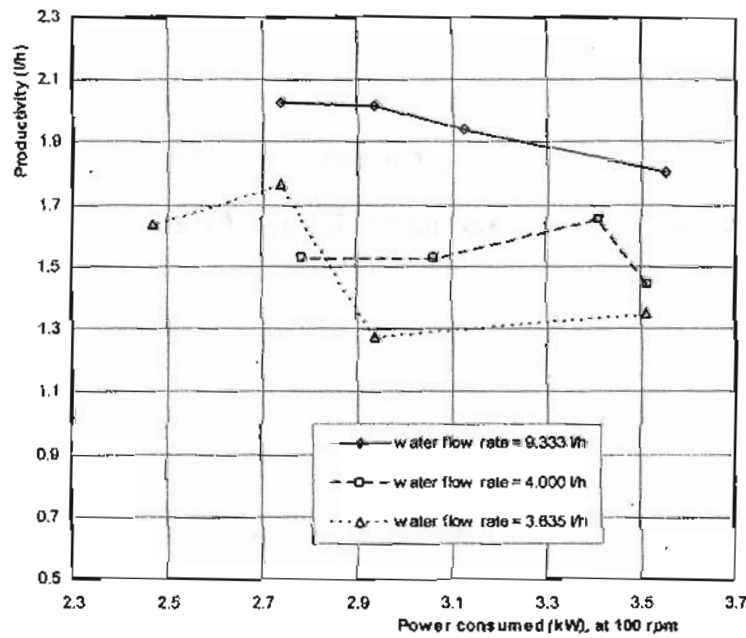

Figure (10) Variation of the system productivity with the power consumed, at 100 rpm for different water flow rates = 9.333, 4.000 and 3.635 l/h
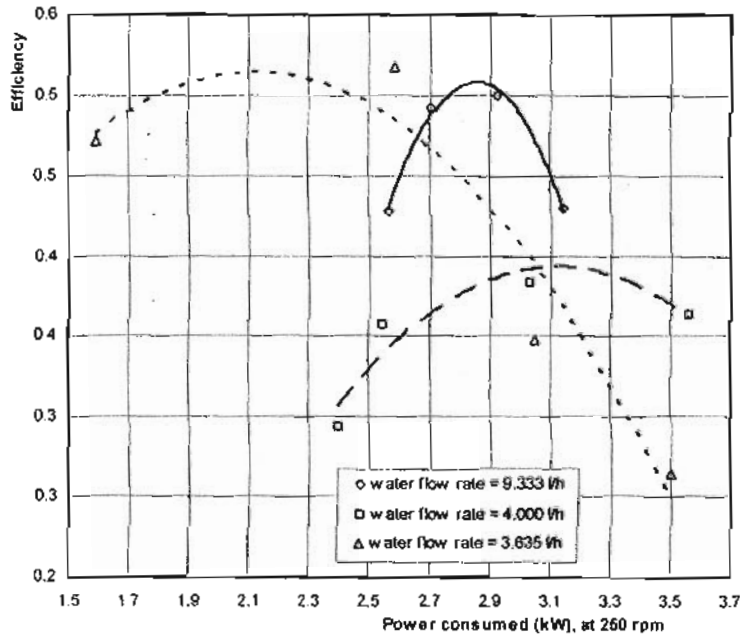
Figure (11) Variation of the system efficiency with the power consumed, at 250 rpm for different water flow rates = 9.333, 4.000 and 3.635 l/h
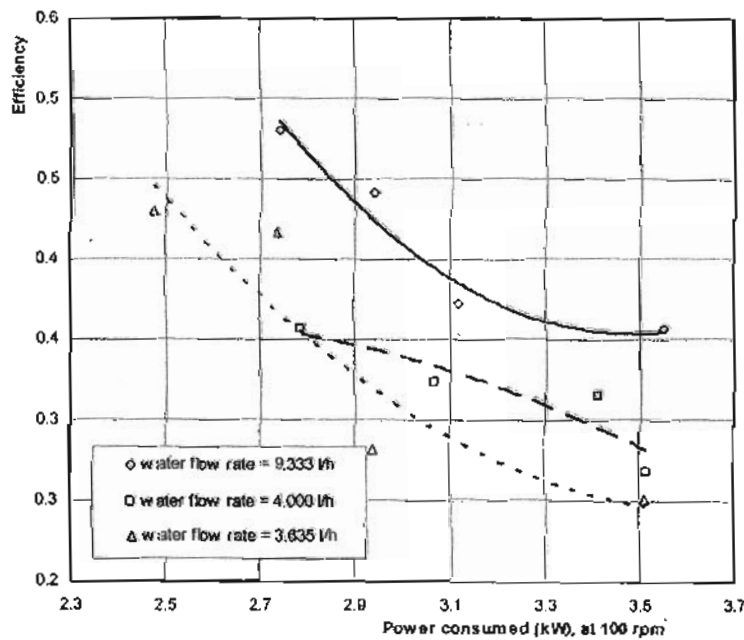

Figure (12) Variation of the system efficiency with the power consumed, at 100 rpm and different water flow rates = 9.333, 4.000 and 3.635 l/h